IRON INFLUENCE IN THE ALUMINOSILICATE ZEOLITES SYNTHESIS

E. I. BASALDELLA,[1] R. M. TORRES SÁNCHEZ AND J. C. TARA[1]

[1] Centro de Investigaciones y Desarrollo en Procesos Catalíticos (CINDECA), La Plata, Argentina
[2] Centro de Tecnología de Recursos Minerales y Cerámica (CETMIC) CC49, 1897 M.B. Gonnet, Argentina

Abstract—The level of Fe impurities in 2 well-crystallized kaolinites was modified (by addition or chemical removal treatment) to analyze the Fe influence in the aluminosilicate zeolite synthesis.

The original and modified clays were heat-treated in order to change their reactivity for zeolite A synthesis, and their thermal transformations were studied by X-ray diffraction (XRD), determination of point of zero charge (PZC) and infrared (IR) techniques. It was established that many structural changes took place, regardless of the Fe clay content. Furthermore, the presence of Fe species in alkaline solution or in the solid phase did not seem to greatly influence the zeolite crystallization, because only small differences in the conversion values among samples with different Fe contents were registered. The crystallization process seemed to be related mainly to Al coordination changes produced by the thermal and Fe removal treatments used.

Key Words—Al Coordination, Iron Influence, Kaolin, Zeolite Synthesis.

INTRODUCTION

The benefits of using kaolin as an aluminosilicate source in zeolite synthesis to obtain lower-cost catalysts, adsorbents or ion exchanger are widely known (Breck 1964, 1974; Howell and Acara 1964; Haden and Dzierzanowski 1968, 1972; Basaldella et al. 1993, 1995; Basaldella and Tara 1995). Unfortunately, it is difficult to find natural kaolins free of impurities, Fe being one of the most usual.

Zeolite A (NaA) is largely utilized as an adsorbent. In the last 10 y, its production has increased 5-fold, mainly due to its use as a polyphosphate substitute in detergent manufacturing (Imbert et al. 1994). For this reason, the concentration of impurities in raw kaolins used to synthesize zeolite NaA was limited in order to fulfill the established specifications in detergent formulation (such as crystallinity, particle size distribution, exchange capacity and whiteness (Llenado 1983). Recent works (Murat et al. 1992) suggested that the kinetics of zeolite crystallization from kaolinite were affected by Fe impurities present in the clay. Nevertheless, other authors (Hamilton et al. 1993), using sodium aluminate and sodium silicate as raw materials, found that the Fe influence in zeolite synthesis was the same as that produced by other solid impurities, such as Mg or Ca, independent of its nature. On this basis, we think that it is worthwhile to study whether the Fe contents of raw kaolins would influence the zeolite synthesis or the thermal activation processes.

Additionally, studies performed by Madani et al. (1990) indicated that the Al coordination number in the raw material played an important role in zeolite conversion from kaolins. This Al coordination was affected by thermal treatment. IR spectroscopy will allow us to determine whether the Al coordination changes with temperature are affected by the Fe content in kaolin.

The aim of the present work is to study the processes of kaolin activation and zeolite crystallization used to obtain NaA zeolite as the main product, and to determine the effect of Fe clay impurities in such processes.

MATERIALS AND METHODS

Two kaolinite samples ("F" from Fisher Company and "C" from Chubut, Argentina) with different Fe content and close crystallinity degrees were chosen as raw materials. Table 1 shows the mineralogical and chemical analyses and Hinckley Index (1963).

To modify the Fe content, 2% of Fe_2O_3 was added to the F (F_{Fe}) sample and the C sample was chemically treated by the dithionite-citrate-bicarbonate method (Torres 1983) to remove Fe (C_{rem}). The C_{rem} sample was water-washed and air-dried. Then 4 series of thermally activated samples were obtained by calcining F, F_{Fe}, C and C_{rem} for 2 h in air at 500, 750, 900 and 980 °C (F_{500}, F_{Fe500}, etc.).

Table 1. Chemical analysis, SiO_2 content and Hinckley Index for initial kaolins.

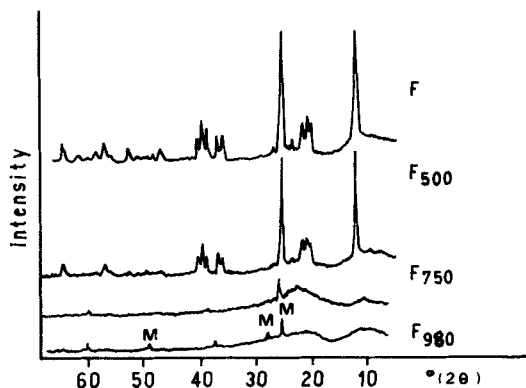| Sample	SiO_2	A_2O_3	Fe_2O_3	TiO_2	H_2O	SiO_2 XRD	Al_2O_3/SiO_2	I_H
C	51.9	34.5	1.9	0.5	12.2	12.0	0.66	0.77
F	42.5	40.8	0.5	2.1	13.9	n.d.	0.96	0.86

Key: n.d. = nondetected.
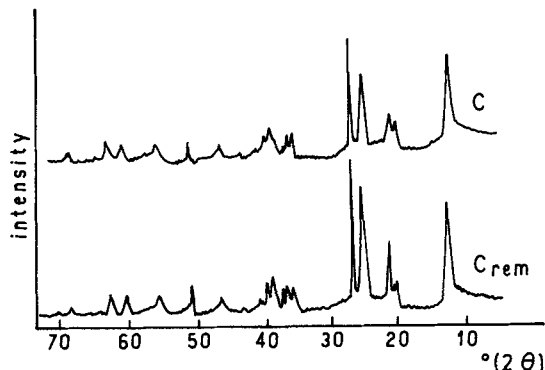
481

Figure 1. XRDs of samples C and C_{rem}.

Figure 2. XRDs of samples F treated thermally.

Zeolite hydrothermal synthesis was carried out at 98 °C in static conditions on mixtures of activated samples, water and NaOH in closed polypropylene containers. NaOH concentrations were chosen to start the synthesis with a molar ratio $Na_2O/Al_2O_3 = 2.5$, appropriate to produce NaA zeolite as the main product.

Solid samples were obtained at different reaction times and the liquid was separated from the solid by centrifugation. The solids, washed until pH = 10 was attained in the wash water, were dried at 110 °C and characterized by XRD analysis using a Philips PW 1732/10 diffractometer and CuKα radiation and Ni filter. The working conditions were 40 kV and 20 mA. Samples were analyzed by the powder mounting technique. Zeolite types obtained were identified by comparing the diffractograms with the standard ones reported in the literature (Breck 1974). Zeolite contents were determined according to the ASTM D-3906/80 method, by considering as 100% the NaA sample of highest conversion.

Solids used in the synthesis were also characterized by IR and PZC determinations (Blok and De Bruyn 1970).

The KBr pellet technique for fine powdered samples was used for determining the IR transmission spectra. The experimental technique was that of pressed pellets, where about 1 mg of clay powder was mixed in with 250–300 mg of KBr powder and pressed at 15,000 psig. Spectra in the region from 200 to 1300 cm^{-1} were obtained using a Bruker IFS66 spectrometer.

The PZC values were obtained by potentiometric titrations, performed on 2 g sample to which 90 mL of 10^{-1} or 10^{-3} M KCl was added as supporting electrolyte. For each experiment, the samples were titrated in N_2 atmosphere with HCl or KOH (0.1 M) with 15-min intervals between each addition. The relative adsorption of proton or hydroxyl ion by the solid sample, reported as μC g^{-1}, was plotted as a function of the pH dispersion. The common intersection point in the potentiometric curves obtained at different electrolyte
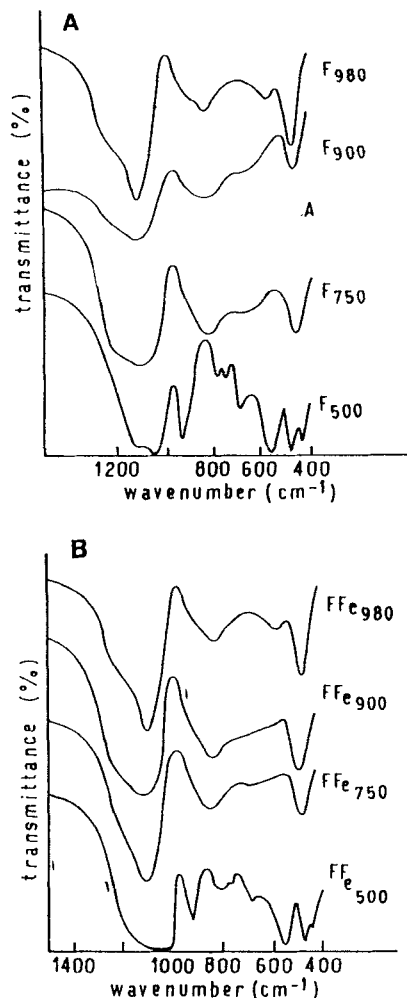

Figure 3. IR spectra for F and F_{Fe} samples treated thermally (A and B, respectively).
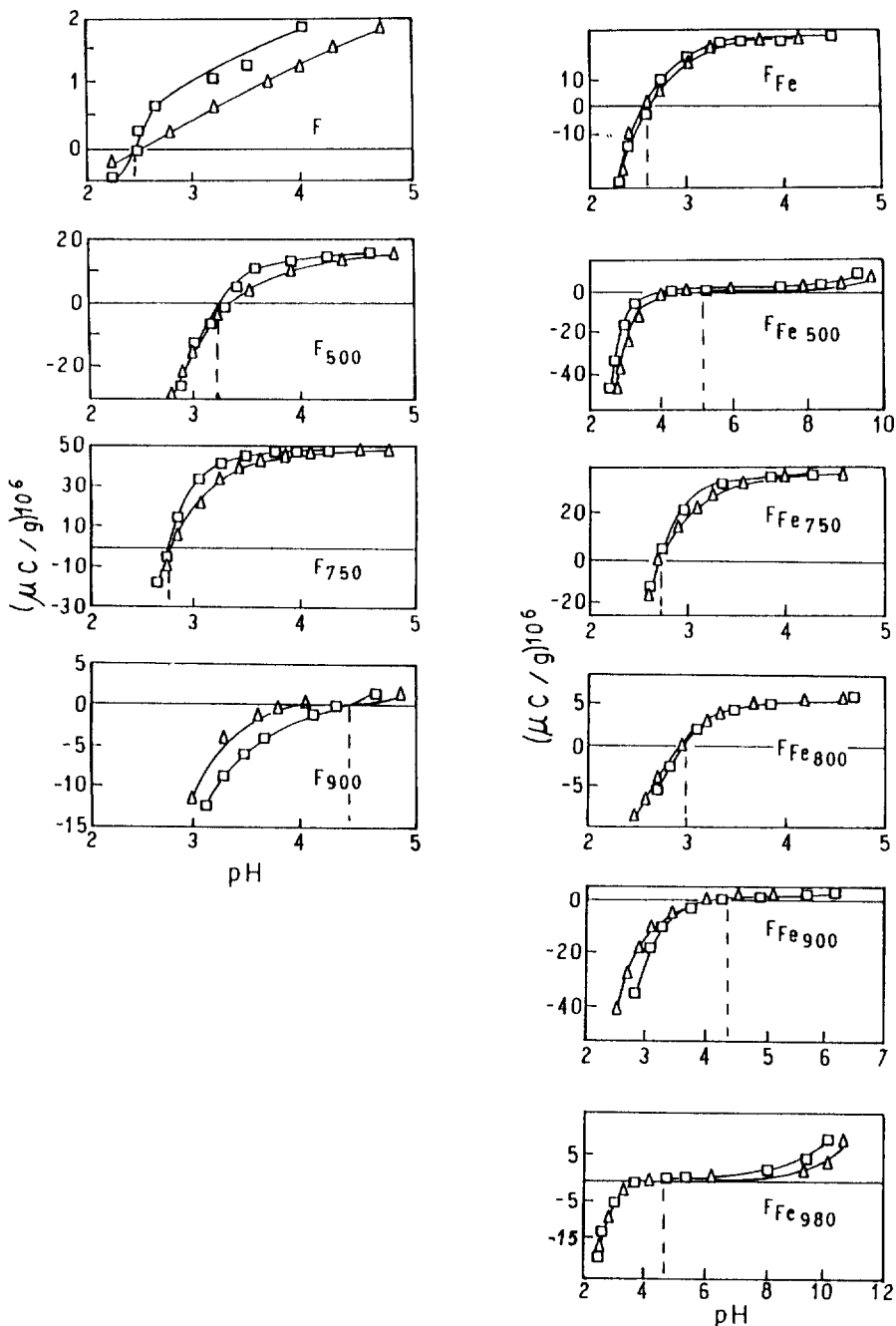
Figure 4.   Potentiometric titration curves of F and F_{Fe} samples treated thermally. Support electrolyte KCl: ($\wedge$) 10^{-1} and ($\square$) 10^{-3} M.

concentrations was considered as the PZC of each sample.

The size and morphology of zeolite particles were determined by scanning electron microscopy (SEM) by means of a Philips SEM 505 equipment. The analyses were performed on gold sputtered powder samples.

RESULTS AND DISCUSSION

Studies on Initial Samples Used for the Hydrothermal Synthesis

XRD AND IR.   X-ray diffractograms corresponding to samples of kaolinite treated chemically and heated at
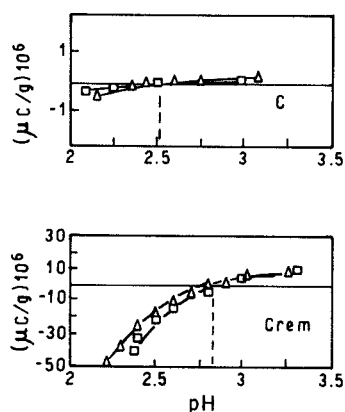
Figure 5. Potentiometric titration curves of C and C_{rem} samples. Support electrolyte KCl: ($\triangle$) 10^{-1} and ($\square$) 10^{-3} M.

Table 2. Hydrothermal synthesis results.

Sample	Zeolite reaction time		A% (XRD) reaction time		A size (μm)
	3 h	10 h	3 h	10 h	10 h
F_{500}	A + HS	trA + HS	—	—	—
F_{750}	A	A	69	96	<3.5
F_{900}	A	A	100	98	<3.0
F_{980}	uX + NaP	NaP	—	—	—
F_{Fe500}	A + HS	trA + HS	—	—	—
F_{Fe750}	A	A	70	83	<3.0
F_{FE900}	A	A	89	86	<3.0
F_{Fe980}	trX + NaP	NaP	—	—	—
					3 h
C_{750}	A	A + HS	100	—	<3.0
C_{rem750}	A	A + HS	49	—	<2.5

Key: tr = traces.

different temperatures are shown in Figures 1 and 2, respectively.

In the C sample (Figure 1), the chemical Fe remotion treatment produced a crystallinity degree decrease (indicated by the Hinckley Index obtained on (111), (110) and (020) peaks), as the result of some clay particle damage produced by the chemical reaction of Na dithionite with structural Al. This occurrence was in agreement with data reported elsewhere (Torres 1983).

With regard to the thermal treatment, temperature increase produced a gradual loss of crystallinity in all series of samples (Figure 2, F series), evidenced by the modification of (111), (110) and (020) peaks up to 750 °C, where the noncrystalline metakaolinite was obtained. At 980 °C, mullite peaks appeared (3.41, 3.21 and 1.84 Å), in agreement with Bulens and Delmon (1977), with the simultaneous silica segregation.

Figure 3 (A and B) shows the IR spectra for F and F_{Fe} series.

IR spectra evolution with temperature for F and F_{Fe} series were identical despite the different Fe contents. In both series, thermal treatment produced a shift in the adsorption band from 537 cm^{-1} (F_{500} and F_{Fe500}) to 800 cm^{-1} (F_{750}, F_{900}, F_{Fe750} and F_{Fe900}), which was in agreement with the octahedral-to-tetrahedral Al coordination change (Madani et al. 1990) and was attributed to kaolinite-metakaolinite transformation (Percival et al. 1974). This tetrahedral Al coordination was stable up to 980 °C, where the 800-cm^{-1} absorption band disappeared and a new band at 550 cm^{-1} occurred, assigned to octahedral Al. The same evolution of IR spectra was observed for the C and C_{rem} series.

PZC MEASUREMENTS. The sensitivity of potentiometric titration curves and the PZC determined from them make it possible to follow the electric surface charge changes due to different initial Fe content and thermal behavior of the kaolin, prior to zeolite synthesis.

Figure 4 shows the potentiometric titration curves of F and F_{Fe} series.

The increase of PZC_{pH} from pH = 2.5 to pH = 3.3 in samples treated up to 500 °C corresponded to the dehydroxylation of the octahedral layer (Tschapek et al. 1974). A further increase of temperature to 750 °C produced a PZC_{pH} decrease to 2.6, which was not consistent with the appearance of tetrahedral Al observed by IR and that would be assigned to a γ-Al_2O_3 formation. The presence of γ-Al_2O_3 would increase the PZC_{pH}, although the formation of a very limited specific surface of γ-Al_2O_3, confirmed by the specific surface reduction from F to F_{750} samples (from 40 to 12.5 m^2/g, respectively) agreed with the pH_{PZC} decrease found (Kuo and Yen 1988). For samples treated at 900 and 980 °C, the PZC_{pH} value was modified by the mullite appearance (as shown in XRD patterns) in agreement with Tschapek (1974) data. The PZC_{pH} of SiO_2 was near 3; therefore, the PZC_{pH} of the mixture (mullite + SiO_2) would be lower than the PZC_{pH} of pure mullite (PZC_{pH} = 8.0) (Smolik 1966).

The 0.1 pH_{PZC} shift of the F_{Fe} sample with respect to the F sample, like the shifts of all F_{Fe} thermal treated samples, indicated the presence of iron oxide added (Pymann et al. 1979).

Figure 5 shows the potentiometric titrations of C and C_{rem} samples.

The C_{rem} sample showed a pH_{PZC} shift of 0.2 towards high pH with respect to the C sample of the pH_{PZC} decrease expected from the Fe removal (0.6% as Fe_2O_3, determined by chemical analyses) (Torres 1983). Also, a higher surface charge density change was observed for C_{rem} with respect to the C sample in the same pH range. These results could be explained by the Al segregation from the kaolinite damaged structure (indicated by the crystallinity decrease). A further coating of the remnant kaolinite by an Al oxyhydroxide layer would produce an increase of the pH_{PZC} in agreement with data obtained previously in ground kaolinite (Torres et al. 1988).

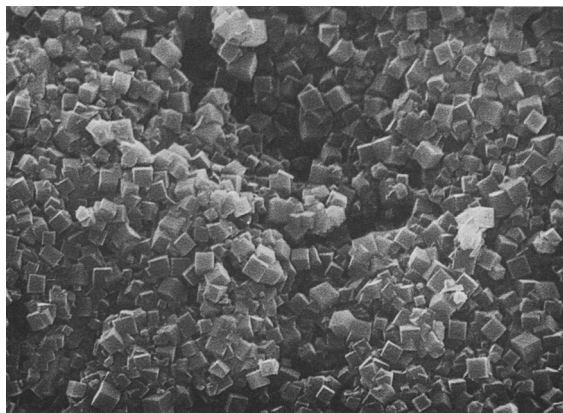HYDROTHERMAL SYNTHESIS. Hydrothermal synthesis results are shown in Table 2.

Figure 6. SEM of the solid product obtained from sample F_{750}. Reaction time 24 h.

In all series of samples, the scanning electron micrographs of the solid products showed cubic crystals of 3 μm sided, on average. Figure 6 depicts this usual morphology of A zeolite for particles obtained from sample F_{750}.

Table 2 shows the rate increase of zeolite A crystallization in F and F_{Fe} samples with temperature treatment, decreasing abruptly at 980 °C. Up to 900 °C, the reactivity was correlated with tetrahedral Al generated by the metakaolinite appearance (as indicated by XRD and IR spectra). As the total kaolinite dehydroxylation occurred at a temperature higher than 840 °C (Murat et al. 1992), the increase obtained in the crystallization rate (from 69 to 100% for F and from 70 to 89% for F_{Fe}) was correlated with the temperature increase from 750 to 900 °C.

When temperature reached 980 °C, a decrease of tetrahedral Al was produced due to pre-mullite structure formation (as indicated by XRD and PZC determinations). This fact modified the effective starting Si/Al ratio for the zeolite synthesis, producing the crystallization of X (NaX), which is a Si-rich structure (Table 2, F_{980} and F_{Fe980} samples). Furthermore, for longer reaction times, the NaX zeolite evolved to the more stable structure of NaP. The transformation of NaX into NaP was completed in 10 h.

For the C series, a decrease of clay reactivity (Table 2, C_{750} and C_{rem750} samples) was observed after the chemical treatment. It could be explained by an octahedral Al removal that took place simultaneously with the Fe remotion (Al_2O_3/SiO_2 = 9%, determined by chemical analyses).

From Table 2 it could be inferred that the zeolite type obtained was temperature-dependent and the Fe content did not play a measurable role.

As the crystallization rate was generally affected by the different cations present in the liquid phase, Fe contents were measured in the supernatant solutions

Table 3. Fe content in the supernatant solution during the crystallization step at different times.

Sample	Fe (ppm)	
	0 h	3 h
F_{750}	15.6	12.8
F_{900}	15.5	15.5
F_{Fe750}	14.9	13.6
F_{Fe900}	16.4	16.2
C_{750}	10.1	9.5
C_{rem750}	8.5	8.1

during the crystallization step, from some samples such as F, F_{Fe} and C (Table 3).

Table 3 shows that the amount of Fe in the supernatant solution slightly differed among samples from the same starting clay.

CONCLUSIONS

Low Fe contents present in the starting clays did not seem to influence zeolite crystallization, notwithstanding a slight decrease in the conversion degree. PZC, IR and XRD studies of initial and thermally treated kaolinites confirmed the gradual kaolinite–metakaolinite transformation, γ-Al_2O_3 and Si_2O with subsequent mullite formation. These transformation were not affected by the presence of varying Fe concentrations in the clay.

The sharp border cubes of 3 μm side characteristic of zeolite NaA crystallites observed by SEM in all samples demonstrated that the nucleation rate was altered neither by the Fe presence nor by thermal treatment. However, the presence of Fe produced a slight decrease of the crystallization rate, as pointed out by Ball et al. (1986).

ACKNOWLEDGMENTS

REFERENCES

Ball J, Dwyer J, Garfdorth AA, Smith W. 1986. The synthesis and characterization of iron silicate molecular sieves. Proc 7th Int Zeolite Conf. p 137–139.

Basaldella EI, Bonetto RD, Tara JC. 1993. Synthesis of NaY zeolite on preformed kaolinite spheres. Evolution of zeolite content and textural properties with the reaction time. Ind Eng Chem Res 32:751–757.

Basaldella EI, Kikot A, Tara JC. 1995. Effect of pellet pore size and synthesis conditions in the in situ synthesis of LSX zeolite. Ind Eng Chem Res. 34:2990–2996.

Basaldella EI, Tara JC. 1995. Synthesis of LSX zeolite in the Na/K system. Influence of the Na/K ratio. Zeolites 11:243–248.

Blok I, De Bruyn PI. 1970. The ionic double layer at the Zn/O solution interface I. The exp. PZC. J Colloid Interface Sci 32:518–525.

Breck DW. 1974. Zeolite molecular sieves. New York: J. Wiley. 313 p.

Breck DW. 1964. US Pat. 3 130 007.

Bulens M, Delmon B. 1977. The exothermic reaction of metakaolinite in the presence of mineralizers. Infl. of crystallinity. Clays Clay Miner 25:271–277.

Haden WL, Dzierzanowski EJ. 1972. US Pat 3 391 994 (1968), 3 503 900 (1972) and 3 657 154.

Hamilton E, Coker EW, Sacco A, Dixon AG, Thompson RW. 1993. The effects of the silica source on the crystallization of zeolite NaX. Zeolites 13:645–653.

Hinckley D. 1963. Variability in crystallinity values among the kaolin deposits of the coastal plain of Georgia and S. Carolina. Clays Clay Miner 13:229–232.

Howell PA, Acara NA. 1964. US Pat. 3 119 660.

Imbert FE, Moreno C, Montero A, Fontal B, Lugano J. 1994. Venezuelan natural aluminosilicates as feedstock in the synthesis of zeolite A. Zeolites 14:374–379.

Kuo JF, Yen TF. 1988. Some aspects in predicting the PZC of composite oxide system. J Colloid Interface Sci 121:220–225.

Llenado RA. 1983. The use of sodium A zeolite in detergents. Olson D, Bisio A, editors. Proc 6th Int Zeolite Conf. p 940–956.

Madani A, Aznar A, Sanza J, Serratosa JM. 1990. Si and Al NMR study of zeolite formation from alkali-leached kaolinites. Influence of thermal activation. J Phys Chem 94:760–765.

Murat M, Amorkrane A, Bastide JP, Montanaro L. 1992. Synthesis of zeolites from thermally activated kaolinite. Some observations on nucleation and growth. Clay Miner 27:119–130.

Percival HJ, Duncan JF, Foster PK. Interpretation of the kaolinite-mullite reaction sequence from IR. J Am Ceram Soc 57:57–61.

Pyman MA, Bowden JW, Posner AM. 1979. The PZC of amorphous coprecipitation of silica with hydrous Al or ferric hydroxide. Clay Miner 14:87–92.

Smolik T, Harman V, Fuerstenau D. 1966. Surface characterization and flotation behaviour of aluminosilicates. Trans Mining Eng AIME 235:367–370.

Torres Sánchez RM. 1983. Etude de l'association entre la kaolinite et le fer externe [thesis]. Belgium: Univ Cathol. de Louvain-la-Neuve, L-1-N. 89 p.

Torres Sánchez RM, Aglietti EF, Porto Lopez JM. 1988. PZC modification on mechanochemical treated kaolinite. Mater Cem and Physics 20:27–38.

Tschapek M, Tcheichvili L, Wasowski C. 1974. The PZC of kaolinite and $SiO_2 + Al_2O_3$ mixtures. Clays Clay Miner 10:219–229.